Published in final edited form as:

J Am Soc Mass Spectrom. 2020 May 06; 31(5): 1093–1103. doi:10.1021/jasms.0c00025.

Structural elucidation of ether glycerophospholipids using gas-phase ion/ion charge inversion chemistry

Caitlin E. Randolph[†], **De'Shovon M. Shenault**[†], **Stephen J. Blanksby**[‡], **Scott A. McLuckey**[†,*]

[†]Department of Chemistry, Purdue University, West Lafayette, Indiana 47907-2084, USA

[‡]Central Analytical Research Facility, Institute for Future Environments, Queensland University of Technology, Brisbane, QLD 4000, Australia

Abstract

Ether lipids represent a unique subclass of glycerophospholipid (GPL) that possess a 1-*O*-alkyl (i.e., plasmanyl subclass) or a 1-*O*-alk-1'-enyl (*i.e.*, plasmenyl subclass) group linked at the *sn*-1 position of the glycerol backbone. As changes in ether GPL composition and abundance are associated with numerous human pathologies, analytical strategies capable of providing high-level structural detail are desirable. While mass spectrometry (MS) has emerged as a prominent tool for lipid structural elucidation in biological extracts, distinctions between the various isomeric forms of ether-linked GPLs has remained a significant challenge for tandem-MS, principally due to similarities in the conventional tandem mass spectra obtained from the two ether-linked subclasses. To distinguish plasmanyl and plasmenyl GPL, a multi-stage (*i.e.*, MS^n where n = 3 or 4) mass spectrometric approach reliant on low-energy collision induced dissociation (CID) is required. While this method facilitates assignment of the *sn*-1 bond type (*i.e.*, 1-*O*-alkyl versus 1-*O*-alk-1'enyl), a composite distribution of isomers is left unresolved, as carbon-carbon double bond (C=C) positions cannot be localized in the *sn*-2 fatty acyl substituent. In this study, we combine a systematic MS^n approach with two unique gas-phase charge inversion ion/ion chemistries to elucidate ether GPL structures with high-level detail. Ultimately, we assign both *sn*-1 bond type and sites of unsaturation in the *sn*-2 fatty acyl substituent using an entirely gas-phase MS-based workflow. Application of this workflow to human blood plasma extract permitted isomeric resolution and in-depth structural identification of major, and in some cases, minor isomeric contributors to ether GPL that have been previously unresolved when examined via conventional methods.

Graphical Abstract

[*]Address reprint requests to: Dr. Scott A. McLuckey, 560 Oval Drive, Department of Chemistry, Purdue University, West Lafayette, IN 47907-2084, USA, Phone: (765) 494-5270, Fax: (765) 494-0239, mcluckey@purdue.edu.

Associated Content

Supporting Information

Additional information discussed in the text that support the presentation of the work (PDF)

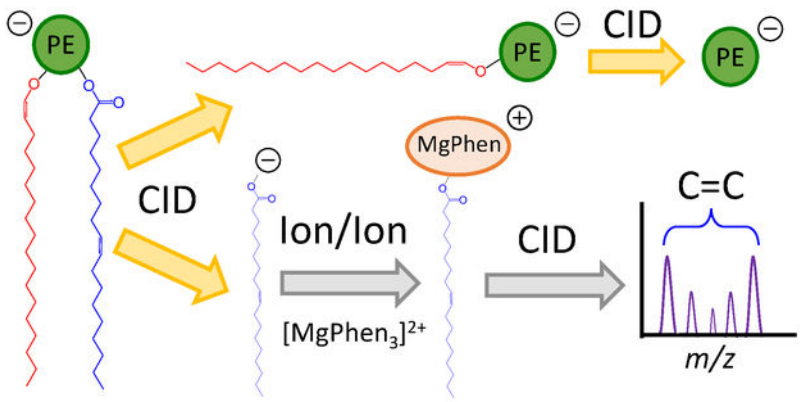

Keywords

ether glycerophospholipids; plasmalogens; ion/ion reaction; charge inversion

Introduction

Ether lipids are peroxisome-derived glycerophospholipids (GPLs) that play significant roles in health and disease.[1, 2] In contrast with the more common diacyl GPL structures, which incorporate two fatty acyl chains esterified at both the *sn*-1 and *sn*-2 positions of the central glycerol backbone, ether-linked GPL are characterized by a hydrocarbon chain linked at the *sn*-1 position via an ether bond. Specifically, while a fatty acid moiety remains esterified at the *sn*-2 position, the plasmanyl and plasmenyl (*i.e.*, plasmalogen) GPL subclasses contain a 1-*O*-alkyl or a 1-*O*-alk-1'-enyl group, respectively, at the *sn*-1 position. Despite constituting only approximately 20% of the mammalian phospholipidome, ether lipids serve diverse structural and functional biological roles.[2] In particular, ether lipids contribute unique structural characteristics to biological membranes, influencing membrane dynamics and physical properties.[3] For example, membrane fluidity is known to be altered by the incorporation of ether-linked GPL, as alkyl chains at the *sn*-1 position permit increased packing efficiency of membrane phospholipids.[3, 4] Furthermore, ether GPL are suggested to function as endogenous antioxidants, while also performing roles in membrane trafficking and cellular signaling.[2,5, 6] Recently, alterations to ether GPL production and composition have been associated with several genetic peroxisomal disorders (*e.g.*, Rhizomelic chondrodysplasia punctata[7], Zellweger syndrome[8]) and multiple common disease pathologies including several types of cancer[9–11], Alzheimer's disease[12], and multiple metabolic disorders (*e.g.*, obesity[13], type 1 diabetes[14], hypertension[15]). In turn, increasing evidence of the critical functional roles of ether lipids in health and disease has highlighted the need for analytical strategies to provide unambiguous structural assignment of these lipids in complex biological mixtures.

Electrospray ionization mass spectrometry (ESI-MS) has emerged as a useful tool to assess changes in GPL structure and composition.[16, 17] However, due to the structural similarities of the two GPL subclasses, differentiation between plasmanyl and plasmenyl GPL represents a major challenge for ESI-MS methods.[18] As conventional lipidomics strategies

like liquid chromatography-mass spectrometry (LC-MS) often fail to achieve chromatographic separation of isomeric ether GPL[19,20], direct infusion ESI-MS (commonly referred to as shotgun lipidomics) has been widely adapted for ether GPL analysis. Following lipid ionization, in either positive or negative ion mode, ether lipids are detected and identified at a sum compositional level via accurate mass measurements (*i.e.*, observed mass-to-charge (*m/z*) ratios).[21] Further structural elucidation can be achieved using tandem-MS (MS/MS).[16] Explicitly, low-energy collision induced dissociation (CID) of mass-selected ether lipid ions permits identification of the polar head group and the fatty acid substituent esterified at the *sn*-2 position. Specifically, GPL classes can be individually detected via exploitation of class-specific fragmentations. For instance, in positive ion mode, glycerophosphocholines (PCs) can be identified using precursor ion scanning of *m/z* 184, while glycerophosphoethanolamines (PEs) are detected via neutral loss (NL) scanning of 141 Da.[22] In negative ion mode, low-energy CID readily cleaves the ester bond at the *sn*-2 position, yielding abundant carboxylate anions reflective of the *sn*-2 fatty acyl constituent. However, in either ion polarity MS/MS alone does not provide direct information regarding the *sn*-1 bond type, as dissociation of the *sn*-1 ether bond is not observed using low-energy CID.[18] Thus, only in specific instances can the *sn*-1 bond type be assigned when exploiting product ion spectra of GPL ions. For example, one can argue that if a monounsaturated ether GPL (*e.g.*, PE *O*-32:1) loses an unsaturated fatty acyl chain from the *sn*-2 position (*e.g.*, loss of 18:1) upon CID of the $[PE - H]^-$ anion, the ether GPL must be a saturated plasmanyl. Aside from this specific case, assignment of GPL subclass can become a difficult task - most notably as the degree of unsaturation increases. In turn, MS^2 product ion spectra are most often insufficient to distinguish an unsaturated alkyl group from a saturated alkenyl moiety at the *sn*-1 position in isomeric ether-linked structures, and thus, most shotgun analyses report ether lipids at the sum compositional level, indicating the need for analytical strategies affording unambiguous ether GPL structural assignment.

Several MS-based approaches have been employed to differentiate GPL subclasses. Widely adopted for plasmalogen identification, Murphy *et al.* described a combination of mild acid hydrolysis and MS/MS.[23] Acid treatment selectively hydrolyzes the labile 1-*O*-alk-1'-enyl bond found in plasmalogens, and thus, direct spectral comparison before and after acid treatment permits identification and differentiation of various subclasses. Despite its usefulness, this approach is inherently destructive and requires multiple analyses of each sample that can act as a constraint on throughput. Alternate solution-based strategies, often in combination with tandem-MS, permit discrimination amongst GPL subclasses. For example, Reid and co-workers developed a selective chemical derivatization of the 1-*O*-alk-1'-enyl bond in plasmalogens that enables confident differentiation amongst GPL subclasses.[24, 25] In a different example, lithium adducted GPL ions (*i.e.*, $[M + Li]^+$), were found to fragment to structurally informative product ions, leading to unambiguous structural assignment.[26] While effective, these approaches are reliant on wetchemical modification prior to MS analysis or ionization of the sample under conditions that do not maximize detection sensitivity. In a multiple-stage ion trap MS approach, Hsu and Turk described an MS^n platform to characterize GPL that facilitates structural differentiation amongst GPL subclasses independent of GPL head group composition.[18,27] Unfortunately, as all methods described above are reliant on low-energy CID, these techniques do not

pinpoint carbon-carbon double bond positions in unsaturated fatty acyl chains at the *sn*-2 position.[17,28] As a consequence, resulting experimental signals likely represent a mixture of unresolved isomers. Failing to clearly define structural features, such as double bond location(s), is problematic, as increasing evidence suggests alterations in lipid isomer relative abundances could serve as sensitive biomarkers for numerous pathologies.[29–32]

While a number of strategies have been established to pinpoint carbon-carbon double bonds in unsaturated lipids, few are capable of identifying the site(s) of unsaturation in intact phospholipids. Furthermore, of these methods, most fail to assign the unsaturation to a particular fatty acyl chain within the complex lipid structure, and in turn, this problem is confounded in ether lipids where different types of carbon-carbon double bond exists (i.e., conventional unsaturation vs. vinyl ether). To our knowledge, only three approaches have demonstrated near-complete ether GPL structure elucidation.[33,34] Specifically, Baba *et al.* used electron impact excitation of ions form organics (EIEIO) to characterize ether GPL extracted from animal tissues.[35] While affording assignment of GPL subclass and the site(s) of unsaturation in radyl substituents, EIEIO ultimately suffers from spectral complexity due a large number of both even- and odd-electron product ions and limited fragmentation efficiency, potentially hindering confident assignment of low abundance lipids or mixtures of isomeric species. The combination of CID with UVphotodissociation in an MS^n workflow can also yield product ions characteristic of acyl chain and double bond positions in GPLs.[36] In an alternate approach, ozone-induced dissociation (OzID) exploits ion/molecule reactions between mass-selected unsaturated lipid ions and ozone vapor within the trapping region of a mass spectrometer to pinpoint carbon-carbon double bond locations.[37] Using OzID and/or a combination of OzID and CID (*i.e.*, OzID/CID), confident, high-level lipid structural identification can be achieved, as only double bond stereochemistry remains unassigned. Nevertheless, ion/ion reactions offer an alternative approach to gas-phase lipid characterization with shorter reaction times leading to potential advantages in duty cycle compared to ion/molecule chemistries.[38–40]

Recently, gas-phase charge inversion ion/ion reactions have been shown to facilitate lipid characterization.[38–41] Betancourt *et al.* exploited charge inversion ion/ion reactions between isomeric singly protonated PC and PE cations (*i.e.*, $[PE + H]^+$, $[PC + H]^+$) and doubly deprotonated dicarboxylic acid dianions to charge invert lipid cations, yielding singly charged lipid anions that can be further interrogated to identify fatty acyl subsituents.[41] Importantly, this approach facilitated chemical separation of isomeric/isobaric PC and PE lipid ions on the *m/z* scale due to distinct reactivities of the lipid cations arising from variations in the polar head group. Thus, mixture complexities from an isolated lipid precursor cation population can be minimized employing ion/ion charge inversion chemistry, further improving mixture analysis performance. In an additional example, charge inversion ion/ion reactions have been shown to provide near-complete structural elucidation of lipids.[38–40] Briefly, fatty acid (FA) anions, derived from non-esterified (*i.e.*, free) FA or complex lipid precursors, are reacted with tris-phenanthroline magnesium complex dications (*i.e.*, $[MgPhen_3]^{2+}$) within the high pressure collision cell of a mass spectrometer to generate charge-inverted FA complex cations (*i.e.*, $[FA - H + MgPhen]^+$). Interrogation of the $[FA - H + MgPhen]^+$ ion facilitates unambiguous isomeric distinction, localization of carbon-carbon double bonds, and in some cases, relative quantitation of isomeric FA.[38,39]

Herein, we report the combination of multiple mass spectrometric workflows to characterize ether GPL. Specifically, we incorporate MS^n experiments with two discrete gas-phase charge inversion ion/ion chemistries to unravel ether GPL molecular structures. In total, the combination of MS^n and ion/ion reactions facilitates in-depth structural identification of ether GPL, including differentiation of plasmenyl and plasmanyl subclasses and assignment of carbon-carbon double bond (C=C) positions within the fatty acyl constituent. Application of the presented method to human plasma extract unveiled ether GPL previously unresolved using conventional approaches. The demonstration of ether lipids present as isomeric mixtures highlights the remarkable structural diversity of these lipid species and the complexity of the human plasma lipidome.

Experimental

Materials

All lipids standards were purchased from Avanti Polar Lipids, Inc. (Alabaster, AL). HPLC-grade methanol, water, acetonitrile, ammonium hydroxide, and chloroform were purchased from Fisher Scientific (Pittsburgh, PA). Magnesium chloride, ammonium acetate, 1,10-phenanthroline (Phen), 1,4-phenylenedipropionic acid (PDPA), and citrated human blood plasma were purchased from Sigma-Aldrich (St. Louis, MO).

Lipid Extraction and Preparation of nESI Solutions

Solutions of lipid standards were prepared in methanol to a final concentration of 5 μM. Magnesium chloride and 1,10-phenanthroline were combined in methanolic solution to a final concentration of 20 μM. A solution of PDPA was prepared at a concentration of ~200 μM in 48.5/48.5/3 (v/v/v) acetonitrile/methanol/ammonium hydroxide. Lipids were extracted from human plasma in an identical fashion as previously described.[40]

Nomenclature

When possible, we adopt the shorthand notation recommended by Liebisch *et al.*[42] For example, glycerophosphoethanolamine and glycerophosphocholine are abbreviated as PE and PC, respectively. In general, 1-*O*-alkyl ether and 1-*O*-alk-1'-enyl ether glycerophospholipids are referred to as the plasmanyl and plasmenyl (plasmalogen) subclasses, correspondingly. Acyl chains are described by the total number of carbons and degree(s) of unsaturation (*e.g.*, 18:1 indicates a fatty acyl chain with 18 carbons and 1 double bond). If known, double bond position and stereochemistry (*Z* for *cis* or *E* for *trans*) are indicated within parentheses following the degree of unsaturation (*e.g.*, 18:1(9Z)). If *sn*-positions are known, radyl substituents are separated by a forward-slash (*i.e.*, PC 16:0/18:1), but if unknown, radyl substituents are separated by an underscore (*i.e.*, PC 16:0_18:1). To indicate ether lipids, proven *O*-alkyl bond (plasmanyl) and *O*-alk-1-enyl bonds (plasmenyl) are indicated with "*O*" and "*P*", respectively. Where an ether linkage is identified but the adjacent carbon-carbon bond cannot be defined, the general "*O*" classification is used. For example, the sum composition PE *O*-36:2 can represent either the plasmanyl PE *O*-18:1(9Z)/18:1 or the isomeric plasmenyl species PE *P*-18:0/18:1(9Z) or a mixture of both.

Mass Spectrometry

All data were collected on a Sciex QTRAP 4000 hybrid triple quadrupole/linear ion trap mass spectrometer (SCIEX, Concord, ON, Canada) with modifications analogous to those previously described.[43] Instrument modifications are illustrated with Supporting Information Figure S1. The essential hardware modification to enable the mutual storage of oppositely charged ions is the application of auxiliary RF signals to the containment lenses of the q2 quadrupole array.

Two types of charge inversion ion/ion experiments were used in this study for lipid characterization. To aid in mixture analysis, the charge inversion approach developed by Betancourt *et al.*[41] was implemented prior to negative ion mode MS^n (Scheme S1). In short, alternately pulsed nESI emitters enable the sequential injection of lipid cations and reagent anions.[44] First, lipid cations were ionized in positive ion mode via direct infusion positive nESI prior to mass-selection in Q1 and subsequent storage in q2. Next, doubly deprotonated reagent PDPA dianions, denoted $[PDPA - 2H]^{2-}$, were ionized in negative ion mode, isolated during transmission through Q1, and accumulated in q2. Once in q2, lipid cations and reagent dianions were reacted under mutual storage conditions for 500 ms. Resulting product lipid anions were then transferred to Q3, isolated using unit resolution, and activated via ion-trap CID (q = 0.25). Product ions generated from CID were analyzed via mass-selective axial ejection (MSAE).[45]

A second experiment employing charge inversion ion/ion chemistry was used to identify sites of unsaturation within the *sn*-2 fatty acyl chain.[40] Direct infusion negative ion nESI was first used to generate the lipid anion. The lipid anion was then isolated during transit through Q1 and sent to the high-pressure collision cell, q2, for storage. Collisional activation of the lipid anion in q2 was employed to generate the *sn*-2 fatty acyl carboxylate anion, denoted $[FA - H]^-$. Now using direct infusion positive ion nESI, the charge inversion reagent dications, $[Mg(Phen)_3]^{2+}$, were generated, mass-selected in Q1, and transferred q2 for storage. In the high-pressure collision cell, reagent dications and product ions resulting from CID of the mass-selected lipid anion were simultaneously stored for 500 ms. Immediately following ion/ion reaction period, all product ions were collisionally activated using beam-type CID and transferred to Q3. Once in Q3, monoisotopic charge inverted FA complex cations (*i.e.*, $[FA - H + MgPhen]^+$) were isolated and activated via single frequency resonance excitation (q = 0.383).

Results

Differentiation of Plasmenyl and Plasmanyl Glycerophospholipids

In negative ion mode, diacyl and ether GPLs can be readily differentiated via MS/MS. However, negative ion mode MS^2 experiments are usually insufficient for distinguishing isomeric plasmenyl and plasmanyl GPL. Specifically, CID of the ether GPL anion predominantly results in cleavage of the *sn*-2 fatty acyl ester bond, revealing structural information pertaining only to the *sn*-2 fatty acyl moiety. As mentioned above, Hsu and Turk developed an MS^n multiple-stage ion-trap MS approach for the characterization of ether lipids.[18,27] Herein, we employ this workflow on a modified hybrid triple quadrupole/linear

ion trap mass spectrometer. Our results are analogous to those previously reported[18,27], noting subtle differences between the data sets, likely due to instrument geometry and resulting differences in ion energetics. Ultimately, we obtained PE subclass differentiation by exploiting MS^3 product ion spectra of the [PE - H - R_2'CH=C=O]ions, while MS^4 product ion spectra of [PC - CH_3 - R_2'CH=C=O]$^-$ permitted identification of PC subclasses, as detailed with Scheme S2. For brevity, results from negative ion mode MS^n experiments are detailed in the Supporting Information (see Figures S2–S3).

While the approach described previously[18,27] was performed exclusively in negative ion mode, PE and PC analysis is often conducted in positive ion mode, as these species yield abundant singly protonated lipid cations upon direct positive ionization. In particular, a common strategy to identify PEs and PCs entails scanning for neutral fragment losses of 141 Da NL scan and *m/z* 184 precursor ions in positive ion mode, respectively. However, interrogation of singly protonated PE and PC cations does not provide information pertaining to acyl chain composition. In turn, lipid cation signals likely represent a mixture of isomeric/isobaric molecular species, as GPL subclass cannot be unambiguously assigned. Notably, isobaric odd chain diacyl and ether GPL cations can be discriminated via high resolution mass analysis. For example, the unambiguous discrimination of the isobaric odd chain diacyl and ether GPL cations such as [PE *P*-18:0/18:1 + H]$^+$ (theoretical *m/z* 730.5745) and [PE 17:0/18:2 + H]$^+$ (theoretical *m/z* 730.5381) can be accomplished if mass resolution exceeds *ca.* 20,000 $M/\Delta M_{FWHM}$. However, differentiation of isomeric ether GPL cations such as [PE *P*-18:0/18:1 + H]$^+$ (theoretical *m/z* 730.5745) and [PE *O*-18:1/18:1 + H]$^+$ (theoretical *m/z* 730.5745) cannot be achieved. Importantly, charge inversion ion/ion chemistry can also be employed to deal with such ambiguities without recourse to high resolution.

To illustrate, synthetic PE *P*-18:0/18:1(9Z), PE *O*-16:0/18:1(9Z), and PE 16:0/18:1(9Z) monocations were subjected to ion/ion reaction with doubly deprotonated PDPA dianions to generate structurally informative [PE - H]$^-$ product ions. We note that isomeric GPL standards of varying subclass are not commercially available, and therefore, we must draw conclusions using the synthetic standards presented herein. Explicitly, mass-selected [PE + H]$^+$ cations undergo charge inversion via double proton transfer to the two carboxylate moieties in doubly deprotonated PDPA to yield [PE - H]$^-$ anions. Results of the ion/ion reaction for PE *P*-18:0/18:1(9Z), PE *O*-16:0/18:1(9Z), and PE 16:0/18:1(9Z) are illustrated in Figure S4, and all cases exhibited a dominant [PE - H]$^-$ production.

The product ion spectra of charge-inverted [PE - H]$^-$ ions derived from synthetic PE *P*-18:0/18:1(9Z), PE *O*-16:0/18:1(9Z), and PE 16:0/18:1(9Z) standards are shown in Figures 1a, 1b, and 1c, respectively. CID of charge-inverted [PE *P*-18:0/18:1(9Z) - H]$^-$ (*m/z* 728.5) yielded an abundant 18:1(9Z) carboxylate anion observed at *m/z* 281.2 and two additional product ions generated via neutral losses of the *sn*-2 fatty acyl moiety as a fatty acid (*i.e.*, [PE *P*-18:0/18:1(9Z) - H - R_2COOH]$^-$, *m/z* 446.3) and as a ketene (*i.e.*, [PE *P*-18:0/18:1(9Z)- H - R_2'CH=C=O]$^-$, *m/z* 464.3) (see Figure 1a). Similarly, interrogation of [PE *O*-16:0/18:1(9Z) - H]$^-$ (*m/z* 702.5) generated via ion/ion reaction gave rise to the [18:1(9Z) - H]$^-$ (*m/z* 281.2) and [PE *O*-16:0/18:1(9Z) - H - R_2'CH=C=O]$^-$ (*m/z* 438.3) product ions (Figure 1b). Thus, as low-energy CID primarily results in ester bond cleavage,

MS/MS experiments alone would be inadequate to distinguish isomeric plasmenyl and plasmanyl GPL that differ only in the location of carbon-carbon double bonds in the ether-linked chain. In contrast, the CID spectrum of charge-inverted [PE 16:0/18:1(9Z) - H]$^-$ (*m/z* 716.5) displays prominent [16:0 - H]$^-$ (*m/z* 255.2) and [18:1(9Z) H]$^-$ (*m/z* 281.2) anions, along with the [PE 16:0/18:1(9Z) - H - R_2COOH]$^-$ (*m/z* 452.3) and [PE 16:0/18:1(9Z) - H - R_2'CH=C=O]$^-$ (*m/z* 478.3) product ions (Figure 1c). The examples in Figure 1 clearly demonstrate that ether GPL can be readily differentiated from their diacyl counterparts, as the latter generate abundant fatty acyl carboxylate anions derived from *sn*-1 and *sn*-2 ester bond cleavage. Such negative ion CID analysis can be used to distinguish ether lipids from isobaric odd chain diacyl GPLs (*e.g.*, [PE *P*-18:0/18:1 - H]$^-$ and [PE 17:0/18:2 - H]$^-$) without the requirement for high resolution mass spectrometry.

To assign *sn*-1 bond type in ether PEs, further dissociation of the [PE - H - R_2'CH=C=O]product ion is required.[18] To demonstrate, the [PE *P*-18:0/18:1(9Z) - H - R_2'CH=C=O]$^-$ (*m/z* 464.3) product ion from Figure 1a was re-isolated in the LIT and subjected to ion-trap CID, giving rise to the product ion spectrum depicted in Figure 1d. Dominating the MS^3 product ion spectrum of [PE *P*-18:0/18:1(9Z) - H - R_2'CH=C=O]$^-$ (*m/z* 464.3) is a product ion observed at *m/z* 196.0 that arises from the neutral loss of the *sn*-1 substituent as a vinyl alcohol (-268 Da). Additionally from Figure 1d, the complementary alkoxide product ion [O-CH=CH-$C_{16}H_{33}$]$^-$ is detected at *m/z* 267.2, providing confirmation of the identify of *sn*-1 substituent and the nature of the ether bond at this position. Interrogation of [PE *P*-18:1(9Z) - H -R_2'CH=C=O]$^-$ (*m/z* 464.3) by MS^3 also generated a product ion at *m/z* 403.3 produced via the 61 Da neutral fragment loss of the ethanolamine (head group (*i.e.*,[PE *P*-18:0/18:1(9Z) - H - R_2'CH=C=O - $HOCH_2CH_2NH_2$]$^-$). In comparison, the MS^3 spectOum of [PE *O*-16:0/18:1(9Z) - H - R_2'CH=C=O]$^-$ (*m/z* 438.3) is defined by a doOinant [PE *O*-16:0/18:1(9Z) - H - R_2'CH=C=O - $HOCH_2CH_2NH_2$]$^-$ ion (*m/z* 377.2). Importantly, further dissociatOon of [PE *O*-16:0/18:1(9Z) - H - R_2'CH=C=O]$^-$ (*m/z* 438.3) does not generate a prominent ethanolamine head group product ion at *m/z* 196.0 as previously observed within the CID spectum of [PE *P*-18:0/18:1(9Z) - H - R_2'CH=C=O]$^-$ (*m/z* 464.3) (*cf.* Figu1es 1d and 1e). For completeness, interrogation of the [PE 16:0/18:l(9Z)- H -R_2'CH=C=O]$^-$ (*m/z* 452.3) anion induced cleavage of the *sn*-1 ester bond, yielding an abundant 16:0 fatty acyl carboxylate anion (*m/z* 255.2), as illustrated inFigure 1f. In sum, implementing MS^3 on analogous charge-inverted [PE - H]$^-$ ions that have undergone neutral fragment losses of the *sn*-2 fatty acyl substituent as a ketene yielded significant mass spectral differences, that consequently enabled structural distinction amongst GPL subclasses and confident assignment of the *sn*-1 bond type.

[PC + H]$^+$ cations also can be transformed in the gas-phase via charge inversion in reactions with doubly deprotonated PDPA reagent dianions. Explicitly, the charge inversion reaction between [PC + H]$^+$ cations derived from synthetic PC *P*-18:0/18:1(9Z), PC *O*-16:0/18:1(9Z), and PC 16:0/18:1(9Z) and PDPA reagent dianions gives rise to [PC + PDPA - H]$^-$ adduct anions that can subsequently dissociate via ion trap CID to yield demethylated PC anions (Figure S5).[41, 46] Following the gas-phase transformation of PC monocations, dissociation of the [PC - CH_3]$^-$ ion produces [PC - CH_3 - R_2'CH=C=O]$^-$ ions that can be further probed via ion trap CID, facilitating identification of radyl constituents and subclass discrimination

(see Figure S6). Briefly, ion-trap CID of [PC - CH_3]$^-$ yielded information regarding only the *sn*-2 fatty acyl substituent, and therefore MS^3 product ion spectra would again be insufficient to differentiate isomeric plasmanyl and plasmenyl PCs. Once more, ion-trap CID of mass-selected [PC - CH_3 - R_2'CH=C=O]$^-$ ions derived from PCs facilitated identification of the *sn*-1 bond type. Specifically, the MS^4 spectra of analogous [PC - CH_3 - R_2'CH=C=O]$^-$ ions derived from plasmenyl, plasmanyl and diacyl PCs presented unique mass spectral features paralleling those described above for PE lipids. It is key to note that while the head group product ion observed at *m/z* 196.0 can be exploited to identify plasmenyl PE, the phosphocholine-derived ion detected at *m/z* 224.0 confirms the plasmenyl PC structure (Figure S6).

Importantly, the combination of charge inversion reactions and the negative ion mode MS^n experiments outlined herein offer a number of benefits when compared to the negative ion mode multiple-stage MS approach alone. Namely, the charge inversion strategy relies on the use of positive ionization for lipid analytes. Particularly for PCs, positive ionization can be more efficient, leading to lower detection limits. Second, PC and PE cations undergo distinct charge inversion processes with PDPA reagent dianions due to differences in the polar headgroups (*i.e.*, primary amine for PEs and quaternary ammonium for PCs). In turn, the net result of the charge inversion ion/ion reaction permits chemical separation of isomeric/isobaric PE and PC lipids entirely in the gas phase.[41] Thus, charge inversion ion/ion chemistry reduces mixture complexities arising from isomeric/isobaric interferences within a single isolated precursor cation population, which can enhance complex mixture analysis performance, especially when considered in combination with negative ion mode MS^n experiments outlined herein.

Identification of fatty acyl double bond position(s) in ether GPL

While the MS^n experiments described above afford confident assignment of *sn*-1 bond type, low-energy CID alone cannot localize carbon-carbon double bond positions in radyl substituents. To pinpoint sites of unsaturation in the *sn*-2 fatty acyl moiety, we employ gas-phase ion/ion charge inversion chemistry. Following ionization via direct negative nESI, collisional activation of mass-selected [PE *P*-18:0/18:1(9Z) - H]$^-$ (*m/z* 728.5) liberated the *sn*-2 fatty acyl substituent, generating the 18:1 carboxylate anion. Note that the resulting CID spectrum for [PE *P*-18:0/18:1(9Z)-H]$^-$ was identical to that shown above in Figure 1a. Next, the MS^2 product ions arising from CID of [PE *P*-18:0/18:1(9Z) - H]$^-$ were allowed to react in the gas-phase with [$MgPhen_3$]$^{2+}$ reagent diactions, yielding the product ion spectrum shown in Figure 2a. The ion/ion reaction favored formation of the [18:1(9Z) - H + $MgPhen_2$]$^+$ (*m/z* 665.4) complex cation, but additional [PE *P*-18:0/18:1(92) - H + $MgPhen_2$]$^+$ and [PE *P*-18:0/18:1(92) - H - R_2'CH=C=O + $MgPhen_2$]$^+$ product ions were also observed at *m/z* 1112.7 and *m/z* 848.4, respectively (Figure 2a). Ensuing beam-type (BT) CID, arising from collisions during energetic transfer of ions from q2 to Q3, produced the CID spectrum shown in Figure 2b, characterized by an abundant [18:1(9Z) - H + MgPhen]$^+$ (*m/z* 485.3) product ion. Also depicted in Figure 2b are the[PE *P*-18:0/18:1(9Z) - H + MgPhen]$^+$ (*m/z* 932.6), [PE *P*-18:0/18:1(92) - H - R_2COOH + MgPhen]$^+$ (*m/z* 650.4), [PE *P*-18:0/18:1(9Z) - H - R_2'CH=C=O - CH_2CH_2NH + MgPhen]$^+$ (*m/z* 625.3) and [PE *P*-18:0/18:1(9Z) - H - R_2COOH - CH_2CH_2NH + MgPhen]$^+$ (*m/z* 607.3) product ions. As

described in previous reports[38, 39], CID of charge-inverted FA complex cations enables unambiguous isomeric distinction and confident assignment of double bond position(s) either via direct spectral interpretation or automated spectral matching. In this example, ion-trap CID of [18:1(9Z) - H + MgPhen]$^+$ (*m/z* 485.3) generated a spectral gap, as highlighted by the blue shading in Figure 2c, corresponding with the carbon-carbon double bond position. In particular, the characteristic spectral gap is flanked by product ions arising from carbon-carbon cleavage allylic to the double bond (*i.e.*, *m/z* 331.2 and 387.2) and displays interruption of the usual 14 Da spacing, as the *m/z* difference between product ions at *m/z* 345.2 and 357.2 is 12 Da, confirming the C9=C10 double bond position in the *sn*-2 acyl chain of synthetic PE *P*-18:0/18:1 (9Z). In an identical fashion, the site(s) of unsaturation can be localized in the fatty acyl substituent of plasmanyl PE. This process for PE *O*-16:0/18:1(9Z) illustrated with Figure S7. Furthermore, charge inversion ion/ion chemistry can be employed to pinpoint carbon-carbon double bond positions in unsaturated ether GPL regardless of polar head group composition. This is demonstrated with the analysis of synthetic PC *P*-18:0/18:1(9Z) and PC *O*-16:0/18:1(9Z), as illustrated with Figures S8 and S9, respectively. In total, the combination of MS^n in negative ion mode with charge-inversion and activation of the ester linked fatty acyl chain we achieve confident assignment of the nature of ether linkage at *sn*-1 and the site(s) of unsaturation on the *sn*-2 chain. We note that in the case of plasmanyl lipids, where unsaturation is detected in the ether linked chain but where double bond(s) are not localized at the ether (*e.g.*, PE *O*-18:1(9Z)/18:1(9Z)), this strategy is unable to directly localize sites of unsaturation carried by the *sn*-1 radyl substituent and auxiliary data would be required for full characterization.

Identification of ether lipids in human plasma

As changes in both plasma lipid content and composition have been linked with numerous pathologies, the human plasma lipidome has been extensively explored with aim of identifying lipid biomarkers.[47] Comprised of thousands of distinct lipid molecular structures, the inherent complexity of the human plasma lipidome presents distinct analytical challenges. Unfortunately, LC-based techniques often fail to provide chromatographic separation of isomeric/isobaric plasmenyl and plasmanyl GPL. If chromatographic separation is not achieved, both structural analogues must be reported, leading to structural ambiguity.[19,20] Furthermore, as double bond position(s) cannot be assigned using conventional lipidomics workflows, most plasma lipids are identified only at the sum compositional (*e.g.*, PC *O*-36:2) or molecular lipid level (*e.g.*, PC *O*-18:0/18:2). Thus, it is plausible that reported plasma lipids, including proposed biomarkers, exist not as a single species but as an unresolved mixture of isomeric structures.

In this study, we interrogated two ether-linked GPL previously identified in human plasma at the sum compositional level exploiting class-specific fragmentations (Figure S10). First, we examined the sum composition PE *O*-38:5 detected as a protonated cation at *m/z* 752.5 upon nESI of a human plasma extract (Figure S11). To reduce mixture complexities, mass-selected [PE *O*38:5 + H]$^+$ (*m/z* 752.5) cations were generated by direct infusion positive nESI and subsequently charge inverted in the gas-phase via ion/ion reactions with PDPA reagent dianions to produce lipid anions as summarized above. The resulting ion/ion reaction spectrum shown in Figure 3a reveals the presence of at least two isomeric or

isobaric components present in the original *m/z* 752.5 ion population, as two prominent charge-inverted product ions were observed. Explicitly, the product ion observed at *m/z* 750.5 in Figure 3a corresponds to the singly deprotonated [PE *O*-38:5 - H]anion and likely represents an ion population composed of exclusively of PE lipid(s), while the product ion detected at *m/z* 972.5 signifies the [PC 34:5 + PDPA - H]$^-$ complex anion. Subsequent mass-selection and ion-trap CID of charge-inverted [PE *O*-38:5 - H]$^-$ (*m/z* 750.5) yields the [20:4 - H]$^-$ (*m/z* 303.2), [20:4 - H - CO_2]$^-$ (*m/z* 259.2), and [PE *O*-38:5 - H - R_2'CH=C=O]$^-$ (*m/z* 464.2) product ions which imply the presence of either PE *O*-18:1/20:4 or PE *P*-18:0/20:4 (Figure 3b). These structures are further supported by the absence of 18:0 and 18:1 carboxylate anions. Unfortunately, interrogation of product ion at *m/z* 464.2 shown in Figure 3b could not be conducted due to low signal levels. Relative to PCs, PEs can suffer from ionization suppression in the positive ion mode, leading to the low abundance of the [PE *O*-38:5 + H]$^+$ precursor ion prior to ion/ion reaction. Thus, low product ion abundances are not inherently due to charge inversion, but instead, are related to low ether GPL abundance in plasma extract and/or PE ionization suppression in positive ion mode.

To interrogate the [PE *O*-38:5 - H - R_2'CH=C=O]$^-$ (*m/z* 464.2) product ion and determine the nature of the *sn*-1 linkage, we turn to direct negative MS^n experiments, in which PE ionization will be less prone to ionization suppression. Following direct negative nESI of plasma extract (Figure S11), dissociation of the [PE *O*-38:5 - H]$^-$ ion (*m/z* 750.5) generated product ions analogous to those observed in Figure 3b, yet the CID spectrum obtained in the absence of charge inversion ion/ion reactions contains abundant product ions not originating from the [PE *O*-38:5 - H]precursor ion, suggesting isomeric/isobaric interferences (Figure 4a). For example, the CID spectrum of [PE *O*-38:5 - H]$^-$ ion (*m/z* 750.5) contains a dominant product ion at *m/z* 480.2 (Figure 4a). Re-isolation and ion-trap CID of the product ion at *m/z* 480.2 revealed an abundant [16:0 - H]$^-$ (*m/z* 255.2) carboxylate anion (Figure S12), suggesting that the MS^2 product ion observed at *m/z* 480.2 in Figure 4a likely originated from an isobaric odd-chain diacyl PC (*i.e.*, [PC 13:0_16:0 + OAc]$^-$ adduct ion with theoretical *m/z* 750.5291). Note that this isobaric interference is absent when using charge inversion ion/ion chemistry (*cf.*, Figure 3a and Figure 4a).

To differentiate amongst the PE *O*-18:1/20:4 and PE *P*-18:0/20:4 structures, we applied negative ion mode MS^n. Following CID of [PE *O*-38:5 - H]$^-$ (*m/z* 750.5), the [PE *O*-38:5 - H R_2'CH=C=O]$^-$ (*m/z* 464.2) product ion was isolated in Q3 and subjected to ion-trap CID. Figure 4b illustrates the MS^3 product ion spectrum of [PE *O*-38:5 - H - R_2'CH=C=O]$^-$(*m/z* 464.2). Exploiting the CID spectrum of [PE *O*-38:5 - H - R_2'CH=C=O]$^-$(m/*z* 464.2), the major isomeric contributor proved to be PE *P*-18:0/20:4, as an abundant product ion characteristic of plasmalogen PE was observed at m/*z* 196.0 (Figure 4b**)**. Also observed in Figure 4b are product ions at m/*z* 267.0 and *m/z* 403.2 corresponding to the [O-CH=CH-$C_{16}H_{33}$]$^-$ and [PE *O*-38:5 - H - R_2'CH=C=O - $HOCH_2CH_2NH_2$]$^-$ ions, respectively. Using this approach, it is important to note that we cannot exclude minor isomeric contributions from PE *O*-18:1/20:4 due to the lack of unique product ions indicative of the plasmanyl subclass upon CID of the [PE *O*-38:5 - H - R_2'CH=C=O]$^-$ ion.

Additional minor isomeric components are suggested by the [PE *O*-38:5 - H]$^-$ product ion spectra obtained with and without charge inversion (see Figure 3a and Figure 4b). In

particular, the [22:4 - H]$^-$ (*m/z* 331.2), [22:5 - H]$^-$ (*m/z* 329.2), and [20:3 - H]$^-$ (*m/z* 305.2) carboxylate anions indicate potential minor isomeric contributions from -but not limited to- PE *O*-16:0/22:5, PE *O*-16:1/22:4, PE *P*-16:0/22:4, and PE *P*-18:1 /20:3, Unfortunately, these suggested structures cannot be corroborated via interrogation of the corresponding [PE *O*-38:5 - H - R_2'CH=C=O]$^-$ ion(s), as signal levels were too low.

To pinpoint carbon-carbon double bonds in the *sn*-2 fatty acyl constituent of PE *P*-18:0/20:4, we employed gas-phase ion/ion chemistry. The product ions depicted in Figure 4a were transformed in the gas-phase via ion/ion reaction with $[MgPhen_3]^{2+}$ dications. The product ion spectrum shown in Figure 4c represents the results of the ion/ion reaction and subsequent collisional activation via BT CID. Isolation and ion-trap CID of charge inverted FA complex cations in the LIT permitted unambiguous assignment of unsaturation site(s).[38] Exploiting the [20:4 - H + MgPhen]$^+$ (*m/z* 507.3) product ion spectrum (Figure S13), the major ether structure was confidently assigned as PE *P*-18:0/20:4(5,8,11,14) via spectral matching to an arachidonic acid standard in the previously constructed fatty acid library.[38]

The plasma derived sum composition PC *O*-38:5 was also interrogated in this study. Recently, serum PC *O*-38:5 has been suggested as a potential biomarker for prostate cancer.[48] However, it is likely that this proposed biomarker exists as an isomeric mixture. Once more, charge inversion of the [PC *O*-38:5 + H]$^+$ cation proceeds via ion/ion reaction with PDPA reagent dianions, generating the product ion spectrum displayed in Figure S14a. The ion/ion reaction yields an abundant [PC *O*-38:5 + PDPA - H]$^-$ (*m/z* 1014.7) complex anion likely comprised exclusively of PC lipid(s). Upon collisional activation, [PC *O*-38:5 + PDPA - H]$^-$ (*m/z* 1014.7) fragments to form the demethylated PC *O*-38:5 anion detected at *m/z* 778.6 (Figure S14b). Ensuing dissociation of the product ion at *m/z* 778.6 revealed a dominant [20:4 - H]$^-$ (*m/z* 303.2) anion and [PC *O*-38:5 - CH_3 - R_2'CH=C=O]$^-$ (*m/z* 492.3) ion (Figure 5a). Together, these product ions indicate the presence of either PC *O*-18:1/20:4 or PC *P*-18:0/20:4. The MS^4 product ion spectrum of [PC *O*-38:5 - CH_3 - R_2'CH=C=O]$^-$ (*m/z* 492.3) contains an abundant product ion corresponding to the neutral loss of dimethylamine observed at *m/z* 403.3, indicative of a plasmanyl PC, while the diagnostic plasmenyl ions at *m/z* 224.0 and 267.2 were present only at low abundance in the spectrum (Figure 5b). Consequently, the alkyl ether linked PC *O*-18:1/20:4 was assigned as the major isomeric contributor to the PC *O*-38:5 sum composition in human plasma. Furthermore, PC *P*-18:0/20:4 was identified as a minor isomeric component based on the presence of low abundance MS^4 product ions detected at *m/z* 224.0 (*i.e.*, polar head group ion) and *m/z* 267.0 (*i.e.*, [O-CH=CH-$C_{16}H_{33}$]$^-$). Using ion/ion chemistry (Figure S15), the 20:4 fatty acyl linked at the *sn*-2 position was identified as 20:4(5,8,11,14) via matching to an arachidonic acid reference standard in the fatty acid database.[38] In total, PC *O*-18:1/20:4(5,8,11,14) and PC *P*-18:0/20:4(5,9,11,14) can be assigned as the major and minor isomeric contributors, respectively. While the site of unsaturation in the ether-linked 18:1 chain of PC *O*-18:1/20:4(5,8,11,14) could not be directly determined from these experiments, recent ozone-induced dissociation measurements on plasma derived PC *O*-38:5 find a double bond at the 9-position in the ether-linked chain.[34] Taken together these data suggest a more complete structural assignment for the dominant isomer as PC *O*-18:l(9)/20:4(5,8,ll,14). The [22:4 - H]$^-$ (*m/z* 331.2) and [22:5-H](*m/z* 329.2) fatty acyl anions provide evidence for additional ether PC isomers, but these additional minor isomeric contributors could not be

confidently assigned due to low abundances of the corresponding [PC - CH_3 - R_2'CH=C=O]$^-$ product ions (Figure 5a).

Qualitatively, our findings indicate that despite the presence of a common *O*-38:5 sum composition in PE and PC subclasses in human plasma, the major isomeric contributors vary in *sn*-1 linkage between classes. That is, the plasmenyl-PE (*i.e.*, PE *P*-18:0/20:4(5,8,11,14)) was assigned as the primary isomeric contributor to the PE *O*-38:5 sum composition, while a plasmanyl-PC (*i.e.*, PC *O*-18:1/20:4(5,8,11,14)) represented the dominant isomer of PC *O*-38:5. Collectively, these data allude to the different underlying mechanisms for PC and PE plasmalogen biosynthesis and regulation.[49] Therefore, the method presented herein could provide an increased understanding of plasmalogen biosynthetic pathways and regulatory factors across different cell types or tissues. Furthermore, as demonstrated with the analysis of human plasma PC *O*-38:5, it is evident that biomarkers identified only at the sum compositional level, may very well exist as a mixture of isomeric structures.

Conclusions

In this work, we pair MS^n with two distinct gas-phase ion/ion charge inversion chemistries to facilitate high-level structural elucidation of ether GPL. Performed on a modified hybrid triple quadrupole/linear ion trap mass spectrometer, distinction of ether GPL subclasses is ultimately based on substantial differences in negative ion mode MS^3 (or MS^4) product ion spectra of ions arising from losses of the *sn*-2 fatty acyl substituent as a ketene. In particular, the MS^n (n = 3, 4) product ion spectrum from a plasmenyl GPL is dominated by an alkenoxide anion that represents the radyl moiety at the *sn*-1 position and a product ion generated via the consecutive loss of the *sn*-1 radyl group from the mass-selected [M - H - R_2'CH=C=O]$^-$ precursor anion. Conversely, the plasmanyl GPL MS^n (n = 3, 4) product ion spectrum is characterized by a product ion reflecting the neutral loss of polar head group. The combination of positive to negative charge inversion ion/ion chemistry via gas-phase ion/ion reactions between PC and PE lipid monocations and doubly deprotonated PDPA dianions with the reported negative ion mode MS^n platform enhances mixture analysis performance, reducing complexities arising from isomeric or isobaric interferences. However, as this technique is reliant on low-energy CID, sites of unsaturation cannot be assigned using this tactic alone. Thus, to pinpoint carbon-carbon double bond position(s) in the *sn*-2 fatty acyl moiety, ion/ion charge inversion reactions were employed. Specifically, fatty acyl anions liberated from ether GPL precursor anions were transformed in the gas-phase via ion/ion reaction with charge inversion dications to generate [FA - H + MgPhen]$^+$ complex cations. Predictable fragmentation patterns of charge-inverted FA complex cations permit unambiguous isomeric distinction and confident identification of double bond position(s). The entirely gas-phase shotgun approach presented herein was successfully applied to identify ether GPL extracted from human plasma, ultimately exposing several isomeric contributors. In turn, the combination of MS^n experiments and ion/ion chemistry enabled confident assignment of all major and some minor isomeric contributors present in plasma ether GPL. As demonstrated with the analysis of plasma PC *O*-38:5, a proposed biomarker for prostate cancer, these data reinforce the need for analytical techniques capable of achieving isomeric resolution and facilitating detailed lipid structural assignments in biomarker discovery. More broadly, the method illustrated here has the potential to provide

insight into plasmalogen biosynthetic pathways and regulatory factors dependent on not only head group composition but also biological origin. Lastly, application of the developed approach could advance our understanding of plasmalogen roles in various metabolic processes and pathologies.

Supplementary Material

Refer to Web version on PubMed Central for supplementary material.

Acknowledgments

This work was supported by the National Institutes of Health (NIH) under Grants GM R37-45372 and GM R01-118484. S.J.B. acknowledges project funding through the Discovery Program (DP150101715 and DP190101486) Australian Research Council (ARC).

References

1. Maeba R; Nishimukai M; Sakasegawa S; Sugimori D; Hara H, Plasma/Serum Plasmalogens: Methods of Analysis and Clinical Significance. Advances in Clinical Chemistry, Vol 70 2015, 70, 31–94. [PubMed: 26231485]
2. Dean JM; Lodhi IJ, Structural and functional roles of ether lipids. Protein & Cell 2018, 9 (2), 196–206. [PubMed: 28523433]
3. Paltauf F, ETHER LIPIDS IN BIOMEMBRANES. Chemistry and Physics of Lipids 1994, 74 (2), 101139. [PubMed: 7859340]
4. Han XL; Gross RW, PLASMENYLCHOLINE AND PHOSPHATIDYLCHOLINE MEMBRANE BILAYERS POSSESS DISTINCT CONFORMATIONAL MOTIFS. Biochemistry 1990, 29 (20), 4992–4996. [PubMed: 2364071]
5. Braverman NE; Moser AB, Functions of plasmalogen lipids in health and disease. Biochimica Et Biophysica Acta-Molecular Basis of Disease 2012,1822 (9), 1442–1452.
6. Brites P; Waterham HR; Wanders RJA, Functions and biosynthesis of plasmalogens in health and disease. Biochimica Et Biophysica Acta-Molecular and Cell Biology of Lipids 2004,1636 (2–3), 219–231.
7. Malheiro AR; da Silva TF; Brites P, Plasmalogens and fatty alcohols in rhizomelic chondrodysplasia punctata and Sjogren-Larsson syndrome. Journal of Inherited Metabolic Disease 2015, 38(1), 111–121. [PubMed: 25432520]
8. Schrakamp G; Schutgens RBH; Wanders RJA; Heymans HSA; Tager JM; Vandenbosch H, THE CEREBRO-HEPATO-RENAL (ZELLWEGER) SYNDROME - IMPAIRED DENOVO BIOSYNTHESIS OF PLASMALOGENS IN CULTURED SKIN FIBROBLASTS. Biochimica Et Biophysica Acta 1985, 833 (1), 170–174. [PubMed: 3967038]
9. Messias MCF; Mecatti GC; Priolli DG; Carvalho PD, Plasmalogen lipids: functional mechanism and their involvement in gastrointestinal cancer. Lipids in Health and Disease 2018,17. [PubMed: 29357881]
10. Skotland T; Ekroos K; Kauhanen D; Simolin H; Seierstad T; Berge V; Sandvig K; Llorente A, Molecular lipid species in urinary exosomes as potential prostate cancer biomarkers. European Journal of Cancer 2017, 70, 122–132. [PubMed: 27914242]
11. Chen XL; Chen HK; Dai MY; Ai JM; Li Y; Mahon B; Dai SM; Deng YP, Plasma lipidomics profiling identified lipid biomarkers in distinguishing early-stage breast cancer from benign lesions. Oncotarget 2016, 7(24), 36622–36631. [PubMed: 27153558]
12. Han XL; Holtzman DM; McKeel DW, Plasmalogen deficiency in early Alzheimer's disease subjects and in animal models: molecular characterization using electrospray ionization mass spectrometry. Journal of Neurochemistry 2001, 77 (4), 1168–1180. [PubMed: 11359882]

13. Donovan EL; Pettine SM; Hickey MS; Hamilton KL; Miller BF, Lipidomic analysis of human plasma reveals ether-linked lipids that are elevated in morbidly obese humans compared to lean. Diabetology & Metabolic Syndrome 2013, 5. [PubMed: 23384060]

14. Oresic M; Simell S; Sysi-Aho M; Nanto-Salonen K; Seppanen-Laakso T; Parikka V; Katajamaa M; Hekkala A; Mattila I; Keskinen P; Yetukuri L; Reinikainen A; Lahde J; Suortti T; Hakalax J; Simell T; Hyoty H; Veijola R; Ilonen J; Lahesmaa R; Knip M; Simell O, Dysregulation of lipid and amino acid metabolism precedes islet autoimmunity in children who later progress to type 1 diabetes. Journal of Experimental Medicine 2008, 205 (13), 2975–2984. [PubMed: 19075291]

15. Graessler J; Schwudke D; Schwarz PEH; Herzog R; Shevchenko A; Bornstein SR, TopDown Lipidomics Reveals Ether Lipid Deficiency in Blood Plasma of Hypertensive Patients. Plos One 2009, 4 (7).

16. Pulfer M; Murphy RC, Electrospray mass spectrometry of phospholipids. Mass Spectrometry Reviews 2003, 22 (5), 332–364. [PubMed: 12949918]

17. Blanksby SJ; Mitchell TW, Advances in Mass Spectrometry for Lipidomics. Annual Review of Analytical Chemistry,, Yeung ES; Zare RN, Eds. 2010; Vol. 3, pp 433–465.

18. Hsu FF; Turk J, Differentiation of 1-O-alk-1 ’-enyl-2-acyl and 1-O-alkyl-2-acyl glycerophospholipids by multiple-stage linear ion-trap mass spectrometry with electrospray ionization. Journal of the American Society for Mass Spectrometry 2007,18 (11), 2065–2073. [PubMed: 17913512]

19. Bowden JA; Heckert A; Ulmer CZ; Jones CM; Koelmel JP; Abdullah L; Ahonen L; Alnouti Y; Armando AM; Asara JM; Bamba T; Barr JR; Bergquist J; Borchers CH; Brandsma J; Breitkopf SB; Cajka T; Cazenave-Gassiot A; Checa A; Cinel MA; Colas RA; Cremers S; Dennis EA; Evans JE; Fauland A; Fiehn O; Gardner MS; Garrett TJ; Gotlinger KH; Han J; Huang YY; Neo AHP; Hyotylainen T; Izumi Y; Jiang HF; Jiang HL; Jiang J; Kachman M; Kiyonami R; Klavins K; Klose C; Kofeler HC; Kolmert J; Koal T; Koster G; Kuklenyik Z; Kurland IJ; Leadley M; Lin K; Maddipati KR; McDougall D; Meikle PJ; Mellett NA; Monnin C; Moseley MA; Nandakumar R; Oresic M; Patterson R; Peake D; Pierce JS; Post M; Postle AD; Pugh R; Qiu YP; Quehenberger O; Ramrup P; Rees J; Rembiesa B; Reynaud D; Roth MR; Sales S; Schuhmann K; Schwartzman ML; Serhan CN; Shevchenko A; Somerville SE; John-Williams LS; Surma MA; Takeda H; Thakare R; Thompson JW; Torta F; Triebl A; Trotzmuller M; Ubhayasekera SJK; Vuckovic D; Weir JM; Welti R; Wenk MR; Wheelock CE; Yao LB; Yuan M; Zhao XQH; Zhou SL, Harmonizing lipidomics: NIST interlaboratory comparison exercise for lipidomics using SRM 1950-Metabolites in Frozen Human Plasma. Journal of Lipid Research 2017, 58 (12), 2275–2288. [PubMed: 28986437]

20. Quehenberger O; Armando AM; Brown AH; Milne SB; Myers DS; Merrill AH; Bandyopadhyay S; Jones KN; Kelly S; Shaner RL; Sullards CM; Wang E; Murphy RC; Barkley RM; Leiker TJ; Raetz CRH; Guan ZQ; Laird GM; Six DA; Russell DW; McDonald JG; Subramaniam S; Fahy E; Dennis EA, Lipidomics reveals a remarkable diversity of lipids in human plasma. Journal of Lipid Research 2010, 51 (11), 3299–3305. [PubMed: 20671299]

21. Khalil MB; Hou WM; Zhou H; Elisma F; Swayne LA; Blanchard AP; Yao ZM; Bennett SAL; Figeys D, LIPIDOMICS ERA: ACCOMPLISHMENTS AND CHALLENGES. Mass Spectrometry Reviews 2010, 29 (6), 877–929. [PubMed: 20931646]

22. Brugger B; Erben G; Sandhoff R; Wieland FT; Lehmann WD, Quantitative analysis of biological membrane lipids at the low picomole level by nano-electrospray ionization tandem mass spectrometry. Proceedings of the National Academy of Sciences of the United States of America 1997, 94 (6), 2339–2344. [PubMed: 9122196]

23. Kayganich KA; Murphy RC, FAST-ATOM-BOMBARDMENT TANDEM MASS-SPECTROMETRIC IDENTIFICATION OF DIACYL, ALKYLACYL, AND ALK-1-ENYLACYL MOLECULAR-SPECIES OF GLYCEROPHOSPHOETHANOLAMINE IN HUMAN POLYMORPHONUCLEAR LEUKOCYTES. Analytical Chemistry 1992, 64 (23), 2965–2971. [PubMed: 1463218]

24. Ryan E; Reid GE, Chemical Derivatization and Ultrahigh Resolution and Accurate Mass Spectrometry Strategies for "Shotgun" Lipidome Analysis. Accounts of Chemical Research 2016, 49 (9), 1596–1604. [PubMed: 27575732]

25. Fhaner CJ; Liu S; Zhou X; Reid GE, Functional Group Selective Derivatization and Gas-Phase Fragmentation Reactions of Plasmalogen Glycerophospholipids. The Mass Spectrometry Society of Japan, 2012; Vol. 2.
26. Hsu FF; Turk J, Characterization of phosphatidylethanolamine as a lithiated adduct by triple quadrupole tandem mass spectrometry with electrospray ionization. Journal of Mass Spectrometry 2000, 35 (5), 596–606.
27. Hsu FF; Lodhi IJ; Turk J; Semenkovich CF, Structural Distinction of Diacyl-, Alkylacyl, and Alk-1-Enylacyl Glycerophosphocholines as M-15 (-) Ions by Multiple-Stage Linear Ion-Trap Mass Spectrometry with Electrospray Ionization. Journal of the American Society for Mass Spectrometry 2014, 25 (8), 1412–1420. [PubMed: 24781459]
28. Mitchell TW; Pham H; Thomas MC; Blanksby SJ, Identification of double bond position in lipids: From GC to OzID. Journal of Chromatography B-Analytical Technologies in the Biomedical and Life Sciences 2009, 877 (26), 2722–2735.
29. Zhang WP; Zhang DH; Chen QH; Wu JH; Ouyang Z; Xia Y, Online photochemical derivatization enables comprehensive mass spectrometric analysis of unsaturated phospholipid isomers. Nature Communications 2019,10.
30. Qiu YP; Zhou BS; Su MM; Baxter S; Zheng XJ; Zhao XQ; Yen Y; Jia W, Mass Spectrometry-Based Quantitative Metabolomics Revealed a Distinct Lipid Profile in Breast Cancer Patients. International Journal of Molecular Sciences 2013,14 (4), 8047–8061. [PubMed: 23584023]
31. Razquin C; Toledo E; Clish CB; Ruiz-Canela M; Dennis C; Corella D; Papandreou C; Ros E; Estruch R; Guasch-Ferre M; Gomez-Gracia E; Fito M; Yu E; Lapetra J; Wang D; Romaguera D; Liang LM; Alonso-Gomez A; Deik A; Bullo M; Serra-Majem L; Salas-Salvado J; Hu FB; Martinez-Gonzalez MA, Plasma Lipidomic Profiling and Risk of Type 2 Diabetes in the PREDIMED Trial. Diabetes Care 2018, 41 (12), 2617–2624. [PubMed: 30327364]
32. Mundra PA; Barlow CK; Nestel PJ; Barnes EH; Kirby A; Thompson P; Sullivan DR; Alshehry ZH; Mellett NA; Huynh K; Jayawardana KS; Giles C; McConville MJ; Zoungas S; Hillis GS; Chalmers J; Woodward M; Wong G; Kingwell BA; Simes J; Tonkin AM; Meikle PJ; Investigators LS, Large-scale plasma lipidomic profiling identifies lipids that predict cardiovascular events in secondary prevention. Jci Insight 2018, 3 (17).
33. Deeley JM; Thomas MC; Truscott RJW; Mitchell TW; Blanksby SJ, Identification of Abundant Alkyl Ether Glycerophospholipids in the Human Lens by Tandem Mass Spectrometry Techniques. Analytical Chemistry 2009, 81 (5), 1920–1930. [PubMed: 19186979]
34. Marshall DL; Criscuolo A; Young RS; Poad BL; Zeller M; Reid GE; Mitchell TW; Blanksby SJ, Mapping Unsaturation in Human Plasma Lipids by Data-lndependent Ozone-Induced Dissociation. Journal of The American Society for Mass Spectrometry 2019,1–10. [PubMed: 30430435]
35. Baba T; Campbell JL; Le Blanc JCY; Baker PRS; Ikeda K, Quantitative structural multiclass lipidomics using differential mobility: electron impact excitation of ions from organics (EIEIO) mass spectrometry. Journal of Lipid Research 2018, 59 (5), 910–919. [PubMed: 29540574]
36. Williams PE; Klein DR; Greer SM; Brodbelt JS, Pinpointing Double Bond and sn-Positions in Glycerophospholipids via Hybrid 193 nm Ultraviolet Photodissociation (UVPD) Mass Spectrometry. Journal of the American Chemical Society 2017,139 (44), 15681–15690. [PubMed: 28988476]
37. Thomas MC; Mitchell TW; Harman DG; Deeley JM; Nealon JR; Blanksby SJ, Ozone-induced dissociation: Elucidation of double bond position within mass-selected lipid ions. Analytical Chemistry 2008, 80 (1), 303–311. [PubMed: 18062677]
38. Randolph CE; Foreman DJ; Blanksby SJ; McLuckey SA, Generating Fatty Acid Profiles in the Gas Phase: Fatty Acid Identification and Relative Quantitation Using lon/Ion Charge Inversion Chemistry. Analytical Chemistry 2019, 91 (14), 9032–9040. [PubMed: 31199126]
39. Randolph CE; Foreman DJ; Betancourt SK; Blanksby SJ; McLuckey SA, Gas-Phase lon/Ion Reactions Involving Tris-Phenanthroline Alkaline Earth Metal Complexes as Charge Inversion Reagents for the Identification of Fatty Acids. Analytical Chemistry 2018, 90 (21), 12861–12869. [PubMed: 30260210]

40. Randolph CE; Blanksby SJ; McLuckey SA, Toward Complete Structure Elucidation of Glycerophospholipids in the Gas Phase through Charge Inversion Ion/Ion Chemistry. Analytical Chemistry, 2019.

41. Rojas-Betancourt S; Stutzman JR; Londry FA; Blanksby SJ; McLuckey SA, Gas-Phase Chemical Separation of Phosphatidylcholine and Phosphatidylethanolamine Cations via Charge Inversion Ion/Ion Chemistry. Analytical Chemistry 2015, 87 (22), 11255–11262. [PubMed: 26477819]

42. Liebisch G; Vizcaino JA; Kofeler H; Trotzmuller M; Griffiths WJ; Schmitz G; Spener F; Wakelam MJO, Shorthand notation for lipid structures derived from mass spectrometry. Journal of Lipid Research 2013, 54 (6), 1523–1530. [PubMed: 23549332]

43. Yu X; Jin W; McLuckey SA; Londry FA; Hager JW, Mutual storage mode ion/ion reactions in a hybrid linear ion trap. Journal of the American Society for Mass Spectrometry 2005,16(1), 71–81. [PubMed: 15653365]

44. Liang XR; Xia Y; McLuckey SA, Alternately pulsed nanoelectrospray ionization/atmospheric pressure chemical ionization for ion/ion reactions in an electrodynamic ion trap. Analytical Chemistry 2006, 78 (9), 3208–3212. [PubMed: 16643016]

45. Londry FA; Hager JW, Mass selective axial ion ejection from a linear quadrupole ion trap. Journal of the American Society for Mass Spectrometry 2003,14 (10), 1130–1147. [PubMed: 14530094]

46. Stutzman JR; Blanksby SJ; McLuckey SA, Gas-Phase Transformation of Phosphatidylcholine Cations to Structurally Informative Anions via Ion/Ion Chemistry. Analytical Chemistry 2013, 85 (7), 3752–3757. [PubMed: 23469867]

47. Vvendenskaya O; Wang Y; Ackerman JM; Knittelfelder O; Shevchenko A, Analytical challenges in human plasma lipidomics: A winding path towards the truth. Trends in Analytical Chemistry, 2018; Vol. https://dio.Org/10.1016/i.trac.2018.10.013.

48. Patel N; Vogel R; Chandra-Kuntal K; Glasgow W; Kelavkar U, A Novel Three Serum Phospholipid Panel Differentiates Normal Individuals from Those with Prostate Cancer. Plos One 2014, 9 (3).

49. Nagan N; Zoeller RA, Plasmalogens: biosynthesis and functions. Progress in Lipid Research 2001, 40 (3), 199–229. [PubMed: 11275267]

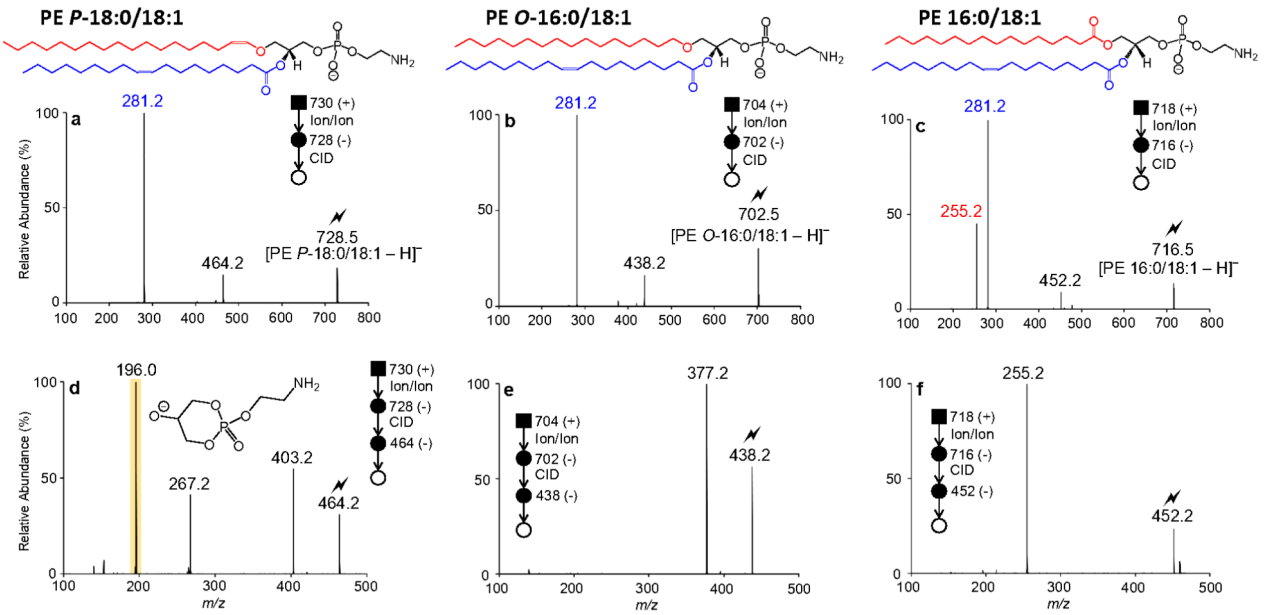

Figure 1.

CID spectra of **(a)** [PE *P*-18:0/18:1(9Z) - H]$^-$ (*m/z* 728.5), **(b)** [PE *O*-16:0/18:1(9Z) H]$^-$ (*m/z* 702.5), and **(c)** [PE 16:0/18:1(9Z)-H]$^-$ (*m/z* 716.5) obtained via charge inversion ion/ion reaction. Product ion spectra obtained via ion-trap CID of mass-selected **(d)** [PE *P*-18:0/18:1 (9Z) - H - R_2'CH=C=O]$^-$ (*m/z* 464.3), **(e)** [PE *O*-16:0/18:1(9Z) - H - R_2'CH=C=O]$^-$ (*m/z* 438.3), and **(f)** [PE 16:0/18:1(9Z) - H - R_2'CH=C=O]$^-$ (*m/z* 452.3). The lightning bolt () indicates the ion subjected to ion-trap CID

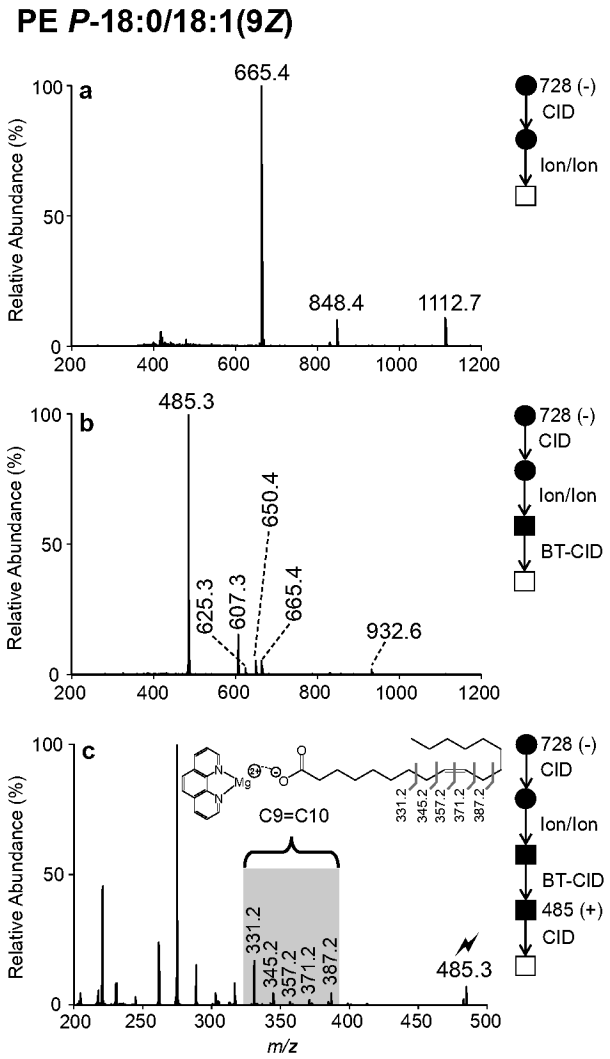

Figure 2.

Demonstration of ion/ion reactions to identify double bond position(s) in the fatty acyl substituent of an unsaturated plasmalogen. **(a)** Product ion spectrum resulting from the ion/ion reaction between $[MgPhen_3]^{2+}$ dications and fragment ions generated via CID of [PE *P*-18:0/18:1(9Z) - H]$^-$. **(b)** Product ion spectrum generated by BT CID of the product ions shown in **(a)**. **(c)** Ion-trap CID spectrum of mass-selected [18:1(9Z) - H + MgPhen]$^+$ (*m/z* 485.3).

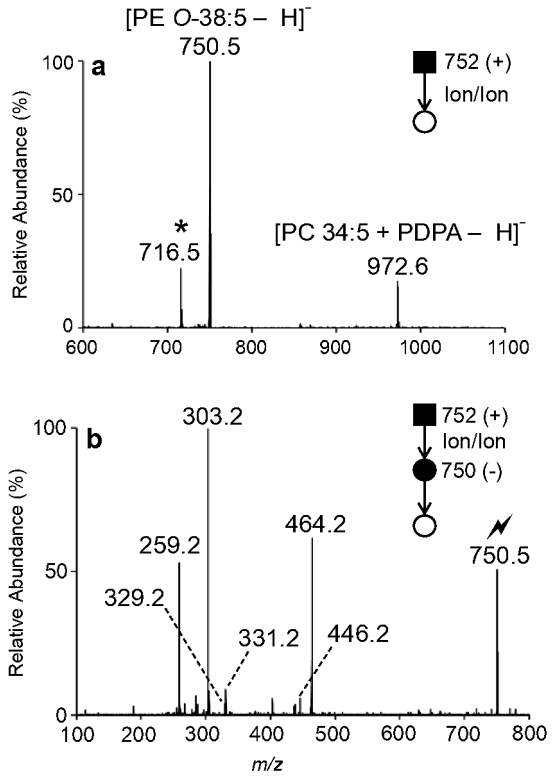

Figure 3.

(a) Mutual storage product ion/ion spectrum resulting from the charge inversion ion/ion reaction of mass-selected $[PE\ O\text{-}38:5 + H]^+$ (*m/z* 752.5) cations and $[PDPA – 2H]^{2-}$ dianions. Note that the mutual storage product ion denoted with an asterisk (*) at *m/z* 716.5 results from the charge inversion of a precursor ion co-isolated with the *m/z* 752.5 cation population. **(b)** MS^3 ion-trap CID spectrum of the ion at *m/z* 750.5 obtained after ion/ion reaction

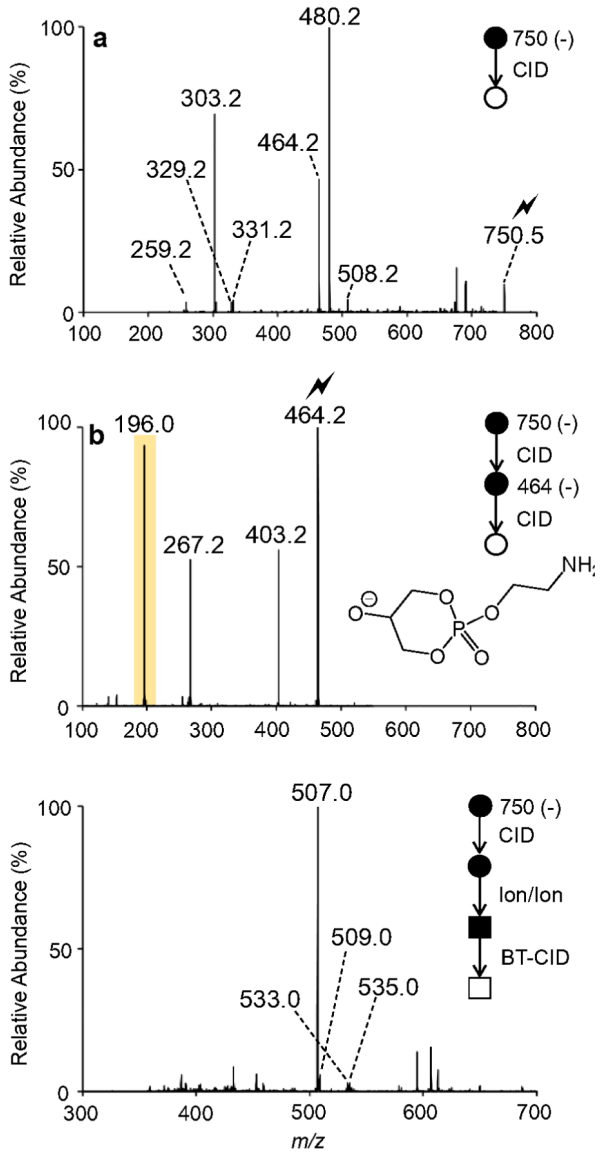

Figure 4.

(a) Ion-trap CID spectrum of the ether-linked PE *O*-38:5 anion at *m/z* 750.5. **(b)** MS^3 product ion spectrum obtained via ion-trap CID of the mass-selected fragment ion observed at *m/z* 464.2 in panel **(a)**. **(c)** Product ion spectrum obtained following the mutual storage charge inversion ion/ion reaction of the fragment ions observed in pane **(a)** with $[MgPhen_3]^{2+}$ dications and subsequent collisional activation with beam-type CID.

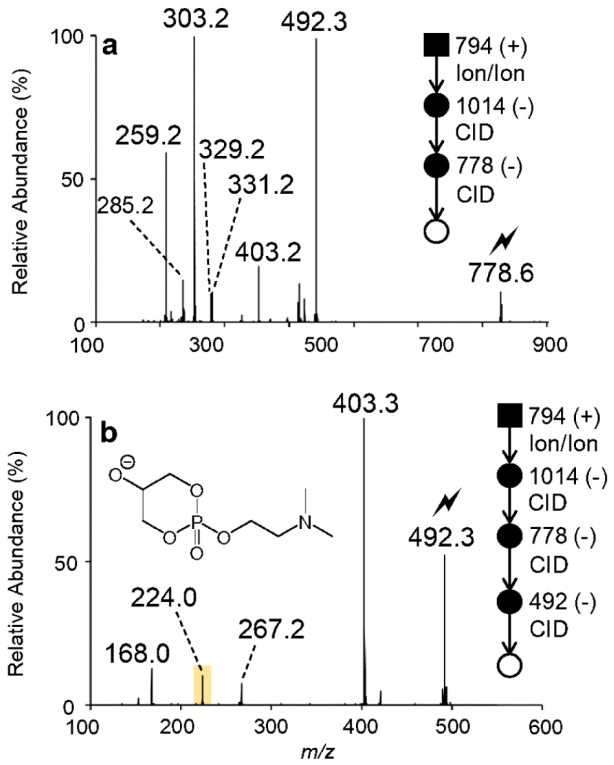

Figure 5.

(a) Product ion spectrum of [PC *O*-38:5 - CH_3]$^-$ (*m/z* 778.6) generated via charge inversion ion/ion reaction of mass-selected [PC *O*-38:5 + H]$^+$ (*m/z* 794.5) cations in human plasma and [PDPA – 2H]$^{2-}$ dianions with subsequent CID of the first generation [PC *O*-38:5 + PDPA H]$^-$ complex anion (*m/z* 1014.7). **(b)** Ion-trap CID spectrum of the ion at *m/z* 492.2 shown in panel **(a)** obtained after ion/ion reaction.